COMPUTATIONAL ANALYSIS OF HYDROGEN DIFFUSION IN POLYCRYSTALLINE NICKEL AND IRREGULAR POLYGONAL MICRO AND NANO GRAIN SIZE EFFECTS

***Jothi, S[1], Croft, T.N.[1], Brown, S.G.R.[1] and de Souza Neto, E.[1]**
[1] College of Engineering, Swansea University, Singleton Park, Swansea, SA2 8PP, UK,
***s.jothi@swansea.ac.uk**

ABSTRACT

The effect of irregular polygonal grain size and random grain boundary on hydrogen diffusion in polycrystalline nickel is investigated. Hydrogen diffusion behavior in micropolycrystalline nickel is compared with that in nanopolycrystalline nickel through numerical analysis. The two dimensional computational finite element microstructural and nanostructural analyses are based on Fick's law corresponding to heterogeneous polycrystalline model geometry. The heterogeneous polycrystalline model consists of random irregular polygonal grains. These grains are divided into internal grain and grain boundary regions, the size of which is determined from the grain size. The computational analysis results show that hydrogen diffusion in nanostructural irregular polycrystalline nickel is higher in magnitude than the microstructural irregular polycrystalline nickel. However, models of voids, traps and micro and nano clustered grains are yet to be included.

1.0 INTRODUCTION

Hydrogen induced embrittlement of single crystal, micropolycrystalline and nanopolycrystalline nickel [1,2,3] is well established as a cause of catastrophic brittle failure and has been studied extensively for more than five decades [1]. Physical factors have been confirmed as one among many factors affecting the hydrogen embrittlement problems. Many physical microstructural factors such as grain size [3] and grain boundary [3] have been identified as playing a vital role for this phenomenon. The processes of hydrogen transport along the microstructural features are essential for understanding the two different modes of hydrogen induced cracking (HIC) in polycrystalline nickel [4, 5]. Intergranular and transgranular failures are two different modes of HIC which are fundamentally different. HIC commonly occurs along grain boundaries where high concentrations of hydrogen can exist [4]. These concentrations highlight the importance of including the random grain boundaries in a model designed to predict embrittlement. Detailed description about the importance of grain boundary diffusion of hydrogen in nickel can be found in Harris [5]. The role of random irregular micro and nano polygonal grains and random irregular grain boundaries plays an active part in the processes of hydrogen diffusion and accumulation mechanism that produces embrittlement failure in nickel [5, 6, 7].

In the present study, the heterogeneous two phase random irregular polygonal grains embedded with random irregular grain boundaries are generated computationally for various micro scale grains with different grain boundaries and nano scale grains with different grain boundaries to study the grain size and intergranular grain boundary effects with respect to the hydrogen diffusion, accumulation mechanism in the micropolycrystalline and nanopolycrystalline nickel.

2.0 HYDROGEN TRANPORTAION EQUATION

The transport of hydrogen as described by Fick's law from the high concentration region to low concentration region based on the equation shown below.

$$J_c(X,t) = -D_{eff}\nabla C = -D_{eff}\left(\frac{\partial c(x,t)}{\partial x} + \frac{\partial c(y,t)}{\partial y}\right) \quad (1)$$

$$J_c(X,t) = -D_{eff}\frac{\partial c(X,t)}{\partial x} \quad (2)$$

The hydrogen flux vector J_c consists of hydrogen concentration gradient $\boldsymbol{\nabla C}$ at a specific time *t* based on *Fick's first diffusion law* by using the *thermodynamic formulation* based on the *Gibbs free enthalpy*. The micro and nano domain microstructural model consists of two phase heterogeneous grain and grain boundary microstructure and the modelling procedure is explained in detail elsewhere [8]. The material properties of the microstructural model are considered as following, the grain hydrogen diffusion coefficient is represented by D_g and the grain boundary hydrogen diffusion coefficient by $D_{gb.}$ Concentration of hydrogen *C*, gradient operator $\boldsymbol{\nabla}$, Laplace operator Δ, *X* represents two dimension (2D) *x,y* directions for simplification. The hydrogen flux vector J_c consists of hydrogen concentration gradient $\boldsymbol{\nabla C}$ at a specific time *t* based on *Fick's first diffusion law* by using the *thermodynamic formulation* based on the *Gibbs free enthalpy*. The micro and nano domain microstructural model consists of two phase heterogeneous grain and grain boundary microstructure and the modelling procedure is explained in detail elsewhere [8]. The material properties of the microstructural model are considered as following, the grain hydrogen diffusion coefficient is represented by D_g and the grain boundary hydrogen diffusion coefficient by $D_{gb.}$

The commercial software ABAQUS implemented the above diffusion equation as shown in (3)

$$J_c(X,t) = -sD_{eff}\frac{\partial \phi(X,t)}{\partial X} \tag{3}$$

Where solubility *s*, $\phi = C/s$ is the normalized hydrogen concentration.

Based on the *law of matter conservation*, the amount of hydrogen is expressed by the continuity equation based on transient (time dependent) diffusion process as described by *Fick's second law*

$$\frac{\partial C}{\partial t} = -div J_c(X,t) \tag{4}$$

$$\frac{\partial C}{\partial t} = D_{eff}\nabla^2 C = D_{eff}\frac{\partial^2 C(X,t)}{\partial X^2} = D_{eff}\Delta C \tag{5}$$

The commercial software ABAQUS solve the governing diffusion equation:

$$\therefore \frac{\partial C}{\partial t} = sD_{eff}\Delta\phi \tag{6}$$

In order to apply (5) in finite element analysis it is converted into the finite element equation given by (7) by applying the discretization.

Element shape function $\boldsymbol{N_j(r)}$ served as trial and weight residual functions, $\boldsymbol{j}$=1,2,3,…,n are number of nodes of the finite element mesh.

$$[M_{ij}]\left\{\frac{dC_j}{dt}\right\} + ([K_{ij}])\{C_j\} = \{F_i\} \tag{7}$$

Where $\boldsymbol{i}$=1,2,3,…,n, {…} represents components vector column, […] represents components element matrices, $[M_{ij}]$ represents the concentration capacity matrix as defined by (8) , $[K_{ij}]$ represents the diffusion matrix (9) and $\{F_i\}$ represents the diffusion flux vector columns given by (10).

$$[M_{ij}] = \int_V N_i N_j dV = \int_V [A]^T [A] dV \tag{8}$$

$$[K_{ij}] = D_{eff}\int \nabla N_i \nabla N_j dV = D_{eff}\int [B]^T [B] dV \tag{9}$$

$$[F_i] = -J_s \int_S N_i dS = \int_S [A]^T J_s dS \tag{10}$$

Where $J_s = D_{eff}\nabla C$,

Where, the interpolation matrixes are [*A*] and [*B*] as shown in (8) to (10).

$$C_j = [A]\{C_j\} \tag{11}$$

$$\frac{dC_j}{dt} = [A]\{\frac{dC_j}{dt}\} \tag{12}$$

$$\nabla C = [B]\{C_j\} \tag{13}$$

The time integration in transient hydrogen concentration $\{\frac{dC_j}{dt}\}$ utilizes the backward Euler method which is also called as modified Crank-Nicholson method is given in (14).

$$\left\{\frac{dC_j}{dt}\right\} = \frac{1}{\Delta t}\left(\{C_j\}_{t+\Delta t} - \{C_j\}_t\right) \tag{14}$$

The resulting discretised from of the governing diffusion equation can be expressed as:

$$\left(\frac{1}{\Delta t}[M_{ij}] + [K_{ij}]\right)\{C_j\}_{t+\Delta t} = \left(\frac{1}{\Delta t}[M_{ij}]\right)\{C_j\}_t + \{F_i\} \tag{15}$$

3.0 IMPLEMENTATION OF MICROSTRUCTURAL AND NUMERICAL MODELLING

Initially the microstructural models are computationally generated with random grain boundaries embedded between irregular random polygonal crystalline grains for both nanopolycrystalline and micro polycrystalline material. The geometric model consists of grains which are composed of three regions: grain interior region, grain boundary region and interface region (i.e exterior of grain boundary which will be shared with the neighbouring adjacent grains). Figure 1 (a) shows a schematic of a grain where the interior is represented by the red colour, the boundary is blue and the interface is the thin green colour. The relative fraction of grain interior region (i.e red colour as shown in the Figure 1 (a)) is smaller in a nanopolycrystalline material and increases in size for a micropolycrystalline material as shown in Figure 1 (b) [9]. The relative fraction of grain boundary region (i.e blue colour in Figure 1 (a)) is higher in nanopolycrystalline material, due to the greater number of relaxed atom in the grain boundary region, and less in micropolycrystalline material, due to reduced number of relaxed atom in grain boundary region. The third region is simply the exterior border part of the grain boundary region which is called as interface (i.e green colour as shown in Figure 1 (a)) and this interface is shared by two adjacent grains in both nanopolycrystalline and micropolycrystalline material as shown in Figure 1 (c) and (d). This interface region doesn't have any physical effect on the model; it is just shown in the schematic view for theoretical explanation in order to get better understanding. More details about this kind of model can be found elsewhere Jothi *et al*. [8] and Meyers *et al.* [9],. Figure1 (c) and (d) show the close up view of computationally simulated model with random irregular grain interiors relative fraction and the random grain boundaries relative fraction between the nanopolycrystalline and micropolycrystalline. Further details can also found in Jothi *et al*. [8].

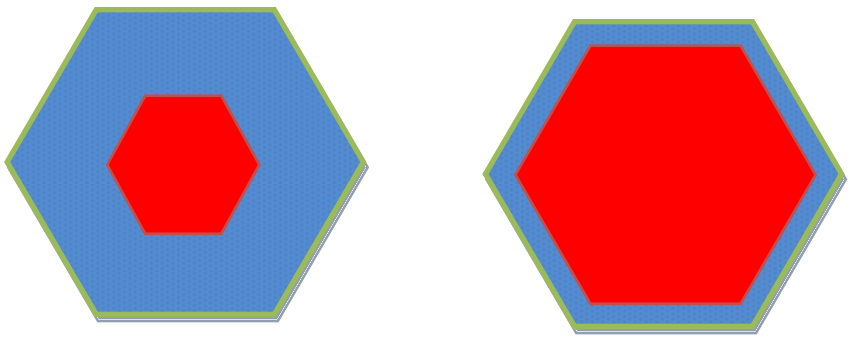

(a) (b)

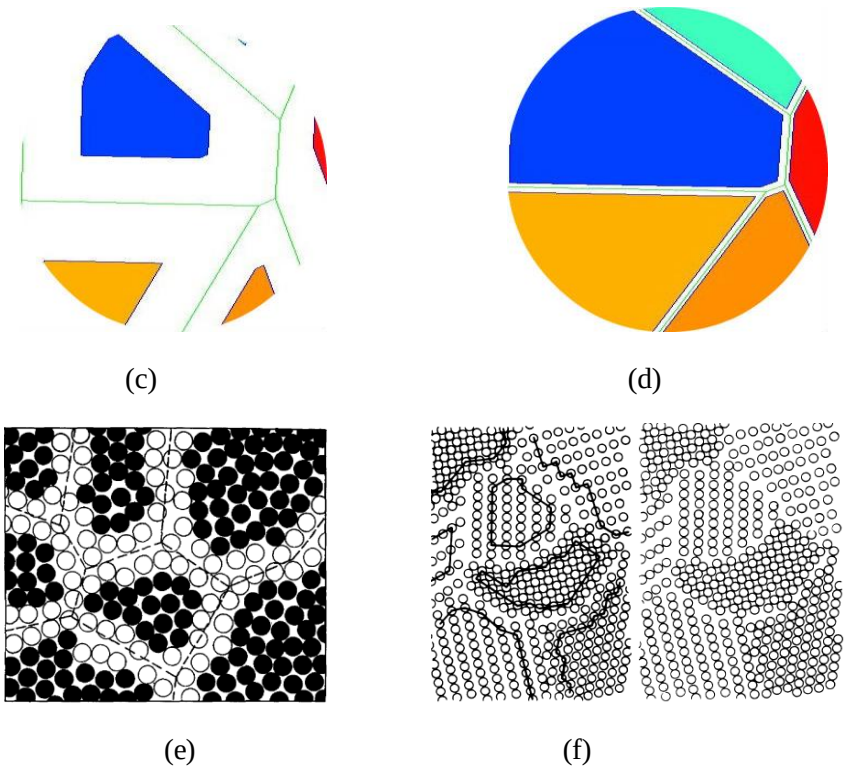

Figure1: Schematic view of relative fraction of grain boundary region (blue colour) and grain interior region (red color) (a) Nanopolycrystalline material [9](b) Micropolycrystalline material [9]. Close up view of computationally simulated models; relative fractions of random grain boundaries (in white colour with shared grain boundary interfaces in green colour) and irregular random polygonal grains interior region in (c) nanopolycrystalline and (d) micropolycrystalline material. (e) Schematic view of two dimensional cross sectional atomic of nanopolycrystalline materials, the atoms with open white circles are grain boundary and the black circles atoms are crystalline grains and the dotted lines are shared grain boundary interfaces between adjustment grains [11]. (f) Two dimensional schematic view of nanocrystalline material in atomic scale with crystalline grain and interfacial grain boundary region separated by the solid lines [14].

The thickness of the embedded random grain boundary region is shared between two adjacent random grains and detailed information can be found in Paggi *et al*. [10]. The micro and nanopolycrystalline material consists of grains where the atoms are in ideal lattice sites and the grain boundary region where the atoms are relaxed away from ideal lattice sites as show in in Figure 1(e) [11]. This kind of model for micropolycrystalline material was initially proposed and implemented for micropolycrystalline nickel by Meyers and Ashworth [12] to investigate the mechanical analysis and then extended to nanopolycrystalline materials by Benson *et al*. [13]. Figure 1(f) shows the two dimensional schematics views of nanocrystalline material at the atomic scale with grain and grain boundary region separated by solid lines Schaefer *et al*. [14]. Micropolycrystalline materials with different grain sizes and different grain boundary thickness were modelled by increasing the relative fraction of grain boundary region as shown in the Figure 2. The domain used for the micropolycrystalline material is 2000 μm*2000 μm and the approximate number of micro scale grains in this domain is around 400. Nanopolycrystalline materials with nano scale grain sizes were modelled by increasing the relative fraction of grain boundaries region with two different domain size, first domain size is 2000 nm*2000 nm (i.e 2 μm*2 μm) and second domain is 2000 nm*20000 nm (i.e 2 μm*20 μm) as shown in Figure 3. The approximate averages number of grains in 2000 nm*2000 nm nanopolycrystalline

S.no.	Simulated microstructural model with micro polycrystalline aggregates	Close view of Irregular random grains and the Area fraction of grain boundary	Random grain boundary networks with mesh
(a)	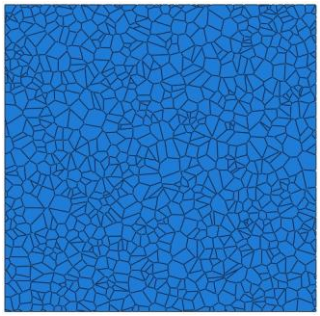	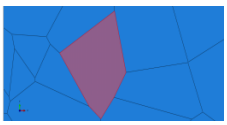	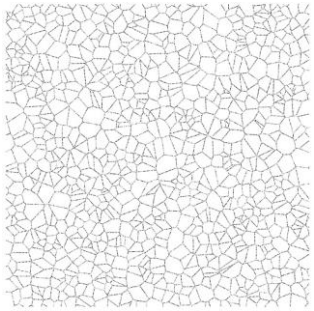
(b)	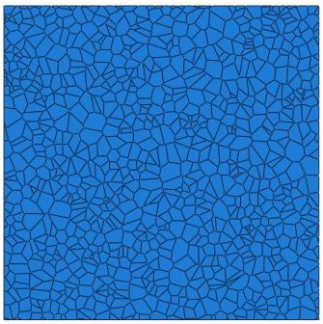	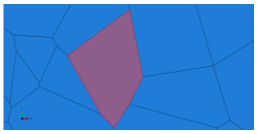	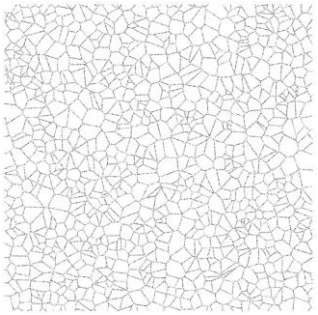
(c)	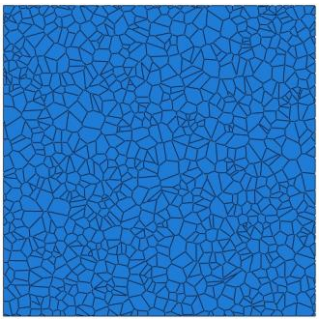	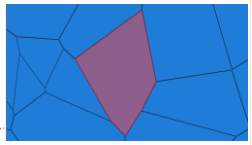	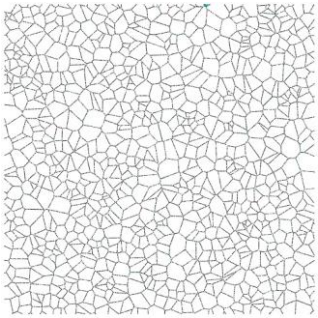
(d)	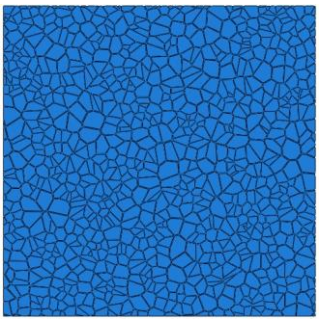	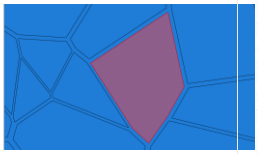	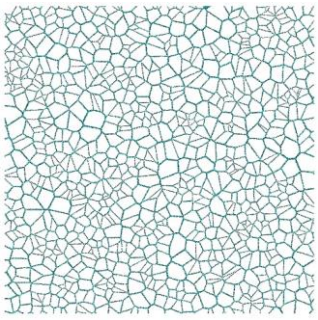

Figure 2. Computationally generated microstructural model with random irregular micro scale polygonal grains and random grain boundary networks in a domain (2000 μm *2000 μm). The average grain size decreases from (a) to (d) and the random average grain boundary thickness increases by one order from (a) to (d).

S.no.	Simulated nanostructural model with nano polycrystalline aggregates	Close view of Irregular random grains and the area fraction of grain boundary	Random grain boundary networks with mesh/ grains
(a)	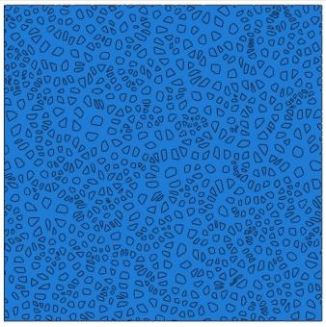	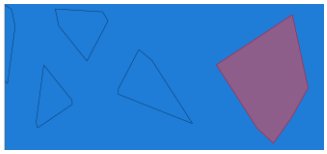	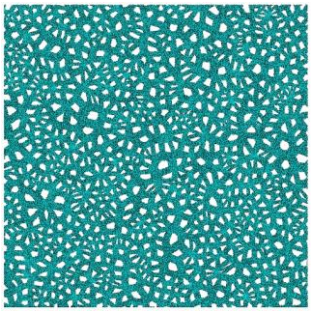
(b)	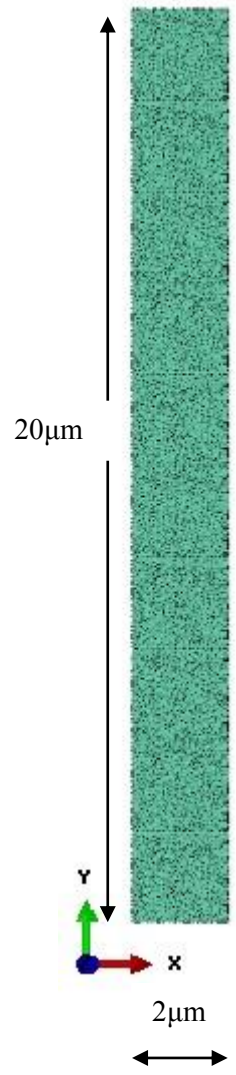	Close view of grain and grain boundary 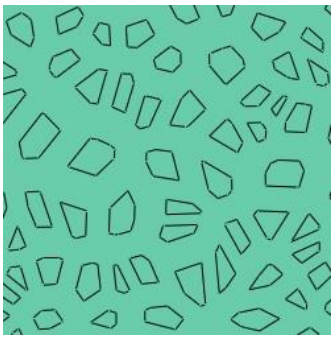 Closed view of grain and mesh 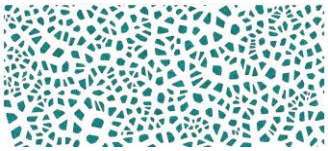 Very close view of nano grains and triangle mesh 	 Dots are grains

Figure 3. Computationally generated nanopolycrystalline model with random irregular nano scale polygonal grains and grain boundary networks in a domain (a) closer view dimension of 2000 nm*2000 nm (b) 2000 nm*20000 nm

domain is 400 and for domain size 2000 nm*20000 nm is around 4000. The nanopolycrystalline model with nano scale grains and the same domain size as the micropolycryalline model would contain approximately 400 million grains. The computational expense of such a model is considerable with a runtime in the order of weeks on a multi-core desktop machine. In order to reduce the computational requirements the 2000 nm*20000 nm domain size was used for nanopolycrystalline model. The detailed explanation of generating these micropolycrystalline and nanopolycrystalline model of irregular random polygonal grains embedded with random shared grain boundaries with varying thickness can be found in Jothi *et al*. [8]. Convergence test were conducted on the generation of aggregation of grains in a square geometric plane. The material properties of nickel such as diffusion coefficient of grain and grain boundary are used in this hydrogen transport analysis can be found in Jothi *et al.* [8]. The initial conditions were assumed as zero hydrogen concentration in the material. Figure 4 shows the dimensions of micropolycrystalline model and boundary conditions of the hydrogen transport analysis in which hydrogen is transported from top source to the bottom sink and the maximum normalized hydrogen concentration is 1 ppm. Another nanopolycrystalline model with dimension 2 µm*20 µm was also considered for the study. The model was meshed with mesh size determined by the mesh convergence tests using linear triangular elements. The simulation of hydrogen diffusion was analysed for the micropolycrystalline model with time periods of 1 sec, 1 hour and 1 day for the different micro scale grain sizes and for different domains. The hydrogen diffusion analysis is simulated for nanopolycrystalline model with nano scale grains for two different domains grain boundary thickness and for nanocrystalline model with the time period of 1 sec.

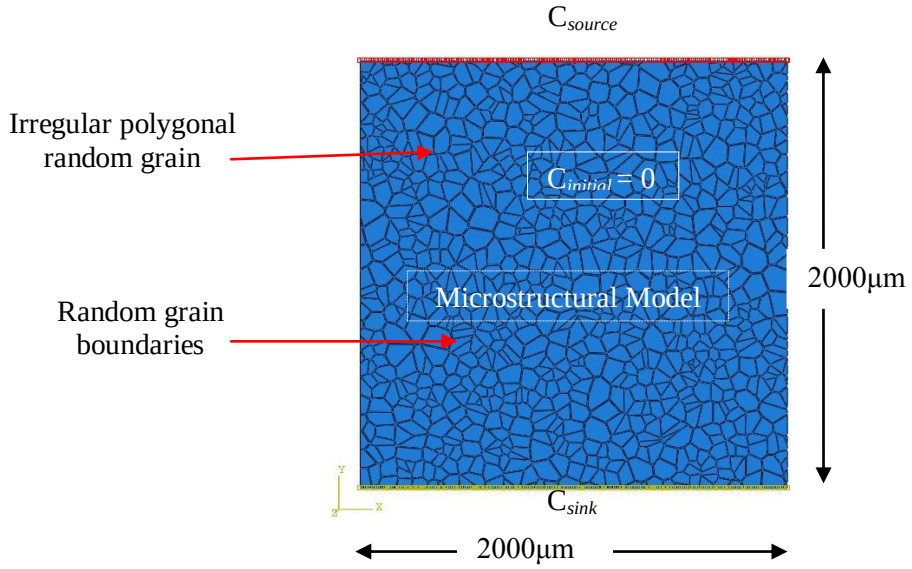

Figure 4. Dimension and boundary condition (hydrogen source in top shown in red colour and hydrogen sink shown in the bottom in yellow colour) of microstructural model with irregular random polygonal grains and random grain boundaries

4.0 RESULTS AND DISCUSSION

4.1 Influences of micro and nano grain sizes and on hydrogen diffusion of heterogeneous two phase micropolycrystalline nickel and nanopolycrystalline nickel

Figure 5 shows the computational hydrogen transport analysis results of the hydrogen concentration in computationally simulated heterogeneous two phase grain and grain boundary with micropolycrystalline nickel square specimens. These simulations used the same sized domain and identical grain distributions. They differ in the proportion of each grain assigned to the interior and grain boundary regions. The simulations used proportions that are characteristic of grain sizes from 100 µm (Figure 5 (a)) down to 100 nm (Figure 5 (d)). The grain size that is characterised by each of the simulation changes by an order of magnitude from one row to the next. The results show the influences of microstructural random irregular polygonal grains and relative grain boundary fraction

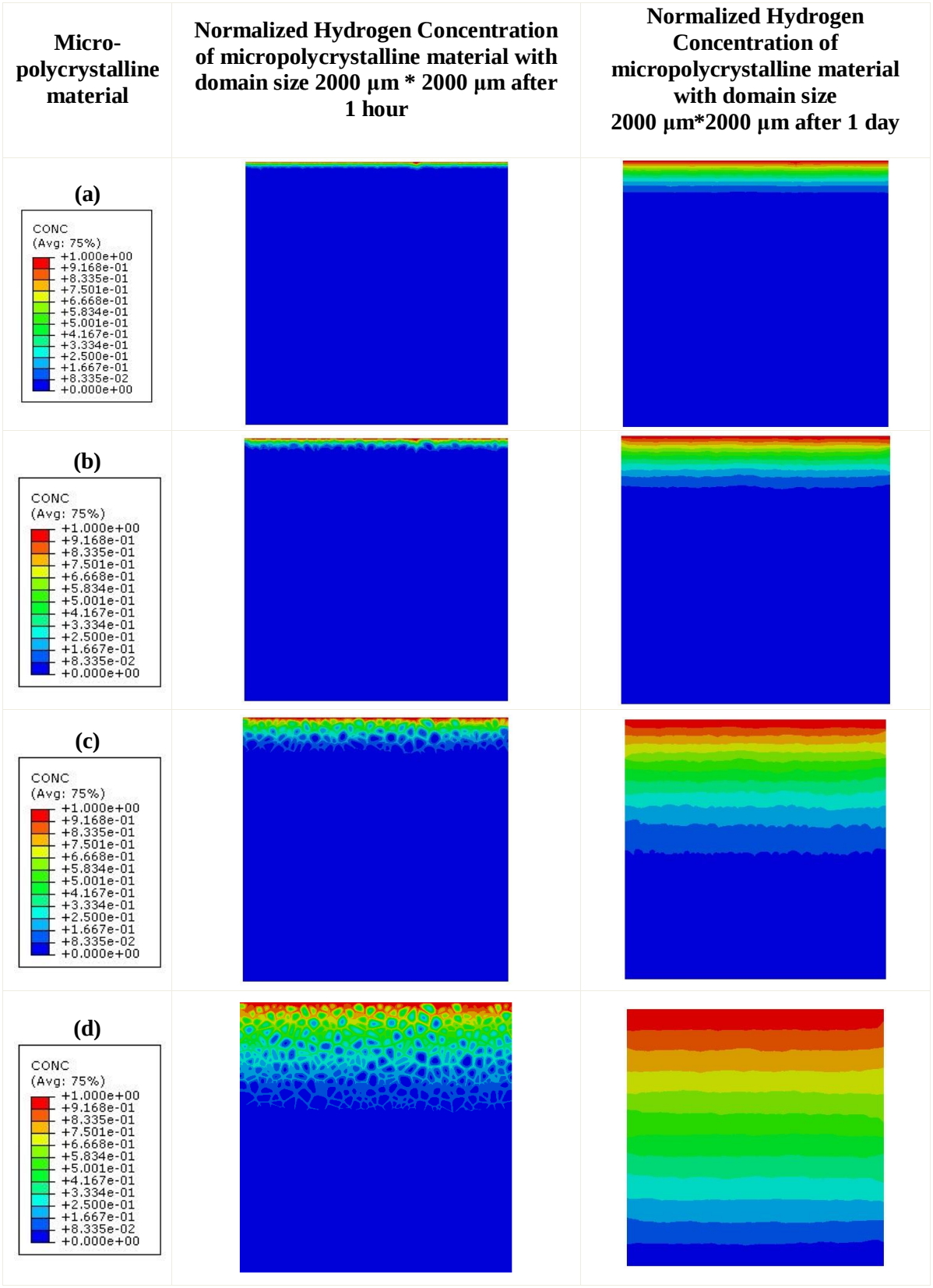

Figure 5. Contours of hydrogen concentration in computationally simulated micropolycrystalline two phase heterogeneous specimen for various grain boundary fractions which are characteristic of decreasing grain size from 100 µm (a) to 100 nm (d) after 1 hour (middle) and 1 day (right).

on hydrogen transport at 25 °C after 1 hour (central column Figure 5) and 1 day (right column Figure 5). The hydrogen diffusion in computationally simulated micropolycrystalline nickel square specimen after the time period of is delayed in the bigger average grain size and accelerated approximately five times the distance in smaller average grain size even with less than one order of grain size as shown in the Figure 5. The hydrogen diffusion in computationally simulated higher relative fraction of grain boundary i.e smaller grain size specimen after the time period of one hour is significantly increased and larger grain size with the grain boundary thickness of one order decreased will hindered approximately half the distance and then strongly delayed approximately one forth the distance for the future increased grain size with the grain boundary thickness of second order decreased. This result shows the influence of relative fraction of grain boundary on hydrogen transport process at 25°C. The results show clearly that decreasing the grain size to the nano scale will increase the bulk diffusion of the nanopolycrystalline material. The results of this analysis reported that bulk hydrogen diffusion process in bigger grain size will be delayed when compared with the smaller grain size polycrystalline nickel.

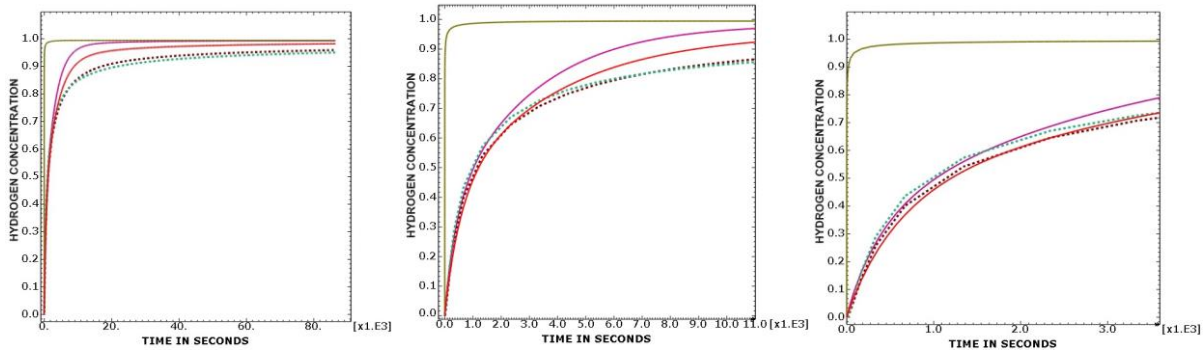

(a) (b) (c)

Figure 6. The hydrogen concentration of micropolycrystalline nickel decreasing one order grain boundary thickness (i.e smaller grain size to bigger grain size) from solid line to dotted line in specified position of various after the following time period. (a) 86400 seconds, (b) 11000 seconds and (c) 3600 seconds.

Figure 6 (a), (b) and (c) shows the predicted hydrogen concentration in micropolycrystalline nickel of various average grain sizes from smaller to bigger (i.e the decreasing relative fraction of grain boundary by decreasing the grain boundary thickness in one order) at 25 °C in the position (i.e all are on grain and green solid line is on grain boundary) of 10 micrometre from the top left corner of the square structure after 86400 seconds, 11000 seconds and 3600 seconds respectively. The comparison between the bigger grain size with smaller grain boundary fraction and smaller grain size with larger grain boundary fraction to the hydrogen concentration corresponding to steady state shows that the hydrogen attains the steady state early in higher relative fraction of grain boundary material which is smaller grain size polycrystalline nickel and the hydrogen takes more time to attain the steady state in smaller relative fraction of grain boundary which is bigger grain size polycrystalline nickel. The hydrogen attains steady state much faster in smaller polycrystalline nickel. Number of studies in literatures already reported that the relative fraction of grain boundary in nanopolycrystalline nickel is significantly larger than the micropolycrystalline nickel [9, 11, and 15]. When we relate this information with the result reported in this study we can justify that the bulk diffusion in nanopolycrystalline nickel will favour higher hydrogen diffusion process that the micropolycrystalline nickel. The hydrogen diffusion in computationally simulated nanopolycrystalline nickel specimen domain 2 μm*20 μm after the time period of 3.27 milliseconds and its close view is shown in the Figure 7(a) and the Figure7 (b) shows the diffusion after the time period of one second. This result shows the inhomogeneous hydrogen diffusion between the grain and grain boundary in the initial stage of the diffusion process is higher.

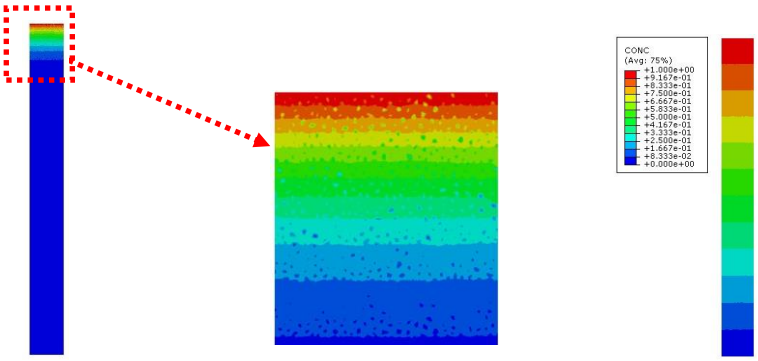

(a) (b)

Figure 7. The hydrogen concentration of nanopolycrystalline nickel domain 2 µm*20 µm (a) after the time period of 3.26 milliseconds and 1 seconds

4.2 Influences of intergranular grain boundary network on hydrogen diffusion of heterogeneous two phase micropolycrystalline and nanopolycrystalline nickel

Even though the interior grain and grain boundary diffusion coefficient in smaller grain size and bigger grain size are same, the computational result observed the diffusion of hydrogen in smaller grain size is increased compared to the bigger grain size polycrystalline nickel at of 25 °C after the same time periods. This enhanced hydrogen diffusion in smaller grain size is due to the increase in contribution of intergranular grain boundary density. The larger density of grain boundary in smaller polycrystalline nickel rapidly increases the hydrogen diffusion along the grain boundary and favours effective bulk hydrogen diffusion in smaller polygonal grains. The intergranular grain boundary density in bigger grained polycrystalline nickel is smaller than the smaller grained polycrystalline nickel. This reduced density delays the effective bulk hydrogen diffusion velocity in the bigger grained polycrystalline nickel. These results confirm the influences of intergranular grain boundary will progressively control the bulk hydrogen diffusion process in micropolycrystalline and nanopolycrystalline nickel.

4.3 Accumulation effects of hydrogen at intergranular grain boundary region in micro and nanopolycrystalline nickel:

The results of the hydrogen diffusion analysis in computationally generated micropolycrystalline for 1 hour and nanopolycrystalline nickel for one second time period is clearly showing that the hydrogen diffusion between the grain interior and grain boundary are inhomogeneous and the diffusion of hydrogen in intergranular grain boundary network is higher than in the polygonal grains which increases the hydrogen flux along grain boundary and accumulates much larger number of hydrogen concentration in the grain boundaries than in the grains as shown in the Figure 8.

(a)

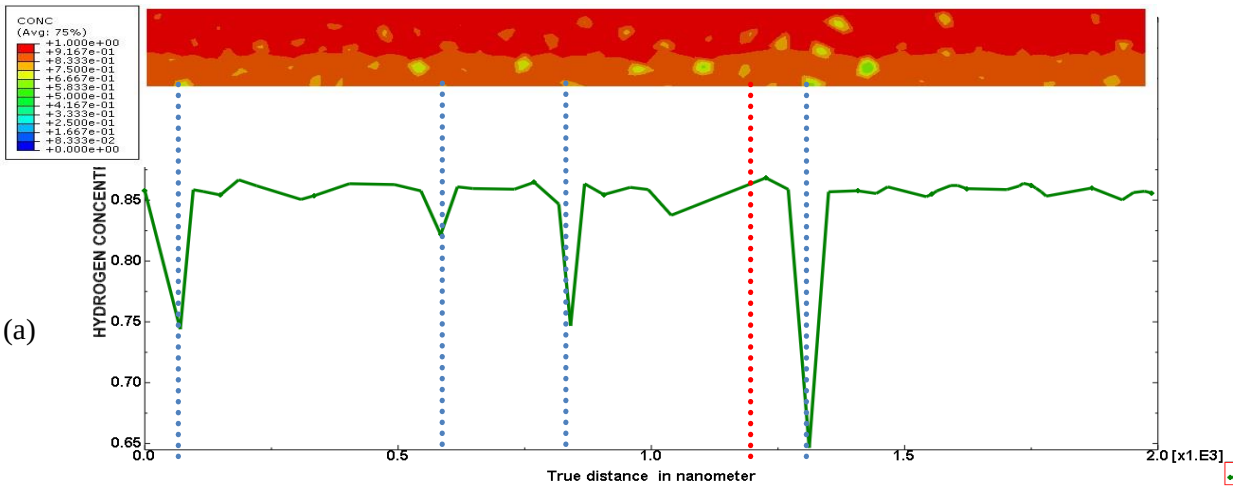

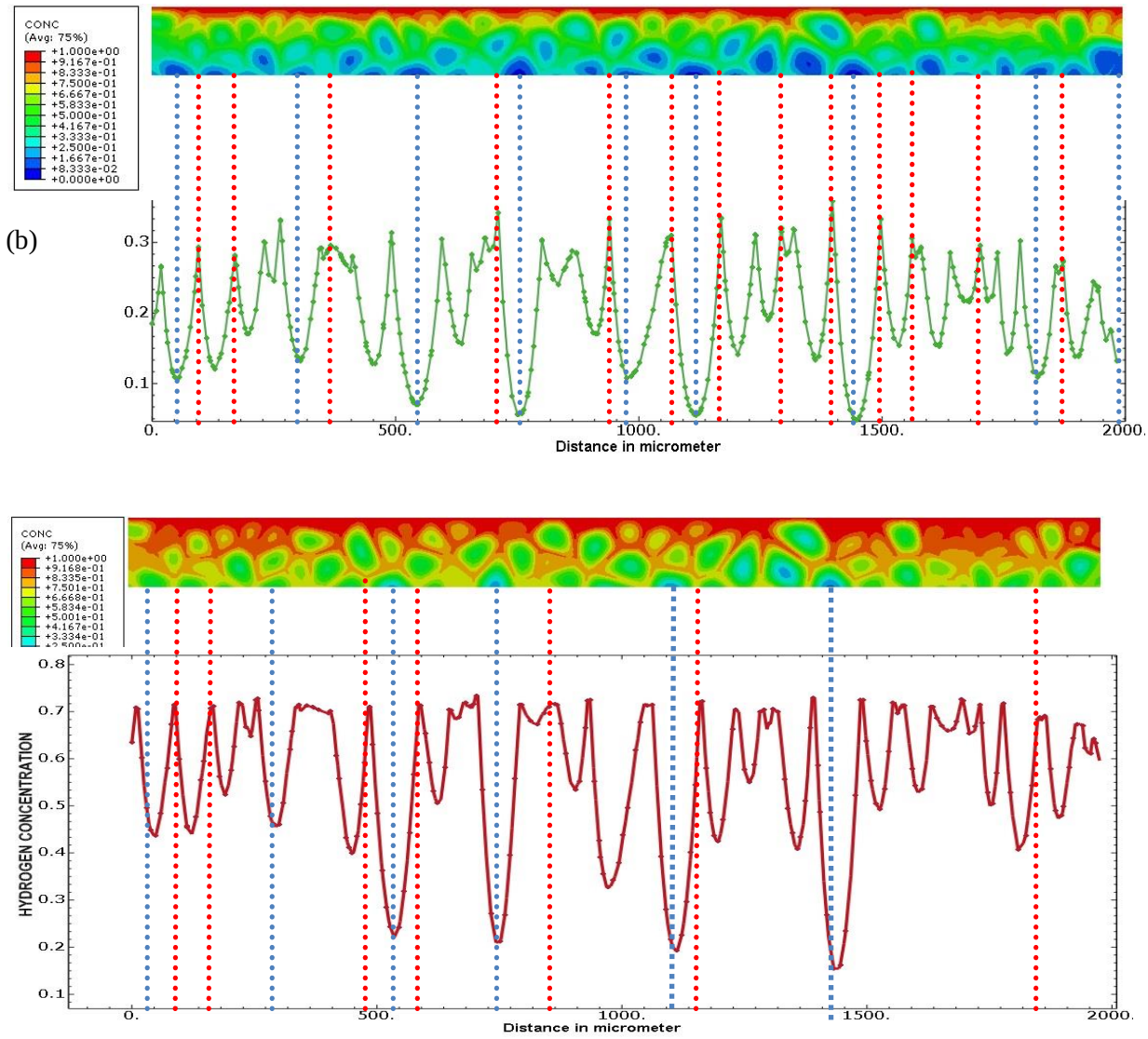

Figure 8. Accumulation mechanism of hydrogen along intergranular grain boundary and inhomogeneous hydrogen diffusion process along grain boundaries and grains for (a) nanopolycrystalline material , (b) micropolycrystalline material with bigger grain size i.e smaller grain boundary relative fraction (c) micropolycrystalline material with higher relative fraction of grain boundary region (smaller micro scale grain size) . (red dotted lines show the accumulation of hydrogen in grain boundaries and blue dotted lines show the hydrogen concentration in grains).

5.0 CONCLUSION

This paper has detailed models of micropolycrystalline and nanopolycrystalline materials with irregular random grains and investigated hydrogen transport by taking into account of nickel material properties. The results of the proposed model demonstrate that the random grain boundaries are high diffusivity paths of hydrogen at room temperature for both the smaller and larger grain sizes. The density of random grain boundaries are higher in smaller grain sized nanopolycrystalline nickel which leads to a faster diffusion of hydrogen in smaller grain sized polycrystalline nickel and nanopolycrystalline nickel. The consequence of this is that the time taken to attain the steady state is much less in smaller grain size polycrystalline nickel and nanopolycrystalline nickel due to its higher relative fraction of grain boundary than the bigger grain size polycrystalline nickel and micropolycrystalline nickel. Hydrogen diffusion and accumulation in micropolycrystalline and nanopolycrystalline between grain and grain boundary are inhomogeneous and much greater hydrogen

concentrations is accumulated in grain boundaries than grains. The hydrogen diffusion and accumulation are higher in grain boundary in smaller and nanopolycrystalline nickel due to its high density of grain boundary than larger and micropolycrystalline nickel. Thus the computation analysis of the proposed model shows the hydrogen transport in polycrystalline nickel is highly sensitive to the physical microstructural factors such as grain sizes and density of grain boundaries and its network. The results also shows the inhomogeneous diffusion and accumulation mechanism of hydrogen between the complex irregular random polygonal grains and random grain boundary in micro and nano scale which can be used as guidance for experimental investigation in order to understand the different modes of the hydrogen induced embrittlement problems in polycrystalline nickel.

Our future work will include the triple junctions, voids, traps and micro and nano clustered grains into the model and apply this model to investigate the stress, temperature, trap and strain assist hydrogen inducted embrittlement problem including hydrogen enhanced localized plasticity and hydrogen assist cracking mechanism.

ACKNOLEDGEMENTS

This work was supported by EU 7th framework program through the project MultiHy (Multiscale Modelling of Hydrogen Embrittlement) under project no. 263335.

REFERENCES

1. Arantes, D.R., Huang, X.Y., Marte, C. and Kirchheim, R., Hydrogen Diffusion and Permeation in Micro- and Nanocrystalline Nickel, *Acta metal. Mater.* , **41**, No. 11, 1993, pp. 3215-3222.
2. Windle, A.H., and Smith,G.C., Metal Sci. J. 12, 1968, pp.187
3. Marte, C., Kirchheim, R., Hydrogen Diffusion in Nanocrystalline Nickel Indicating a Structural Change within the Grain Boundaries After Annealing, Scripta Materialia, 37, No.8, 1997, pp. 1171-1175.
4. Richard, P.G. and Brain, P.S., Gaseous hydrogen embrittlement of materials in energy technologies Volume2: Mechanisms, modelling and future developments, 2012, Woodhead Publishing, Cambridge.
5. Harris,T.M., Latanision.R.M., Grain Boundary Diffusion of Hydrogen in Nickel, Metallurgical Transactions A, 22A,1991, pp.351-355.
6. Brass, A.M., Chanfreau, A., Accelerated Diffusion of Hydrogen along Grain boundaries in Nickel, *Acta Mater*., 44, No.9, 1996, pp.3823-3831.
7. Yao, J. and Meguid, G.A., Hydrogen Diffusion and Intergranular cracking in nickel, Int. J. hydrogen Energy, 22, No.10/11, 1997, pp.1021-1026.
8. Jothi, S., Croft, T.N., Brown,S.G.R. and de Souza Neto, E., Finite Element Microstructural Homogenization techniques and Intergranular, intragranular microstructural effects on effective diffusion coefficient of heterogeneous polycrystalline composite media., Proceedings of the 17th International Conference on Composite Structures, Porto, 17-21 June 2013.
9. Meyers, M.A., Mishra, A., Benson, D.J., Mechanical properties of nanocrystalline materials, Progress in Materials Science, 51, 2006, pp. 427-556.
10. Paggi, M., Wriggers, P., A nonlocal cohesive zone model for finite thickness interfaces-Part II: FE implementation and application to polycrystalline materials, Computational Material Science, 50, 2011, pp.1634-1643.
11. Gleiter, H., Nanocrystalline materials, Progress in Materials Science, 33, 1989, pp.223-315.
12. Meyers, M.A., Ashworth, E., A model for the effect of grain size on the yield stress of metals, Phil. Mag. A, 46, No.5, 1982, pp.737-759.
13. Benson, D.J., Fu, H.H., Meyers, M.A., On the effect of grain size on yield stress: extension into nanocrystalline domain, Materials Science and Engineering, A319-321, 2001, pp.84-861.

14. Schaefer, H.-E., Wurschum,R., Birringer,R., and Gleiter, R., Structure of nanometer-sized polycrystalline iron investigated by positron lifetime spectroscopy, Physical review B, 38, No.14, 1988, pp.9545-9554.
15. Oudriss, A., Creus,J., Bouhattate,J., Conforto,E., Berziou,C., Savall,C., Feaugas,X., Grain size and grain boundary effects on diffusion and trapping of hydrogen in pure nickel, Acta Materialia, 60, 2012, pp.6814-6828.